MNRAS 000, 1–?? (2018) Preprint 22 January 2019 Compiled using MNRAS LaTeX style file v3.0

The expected shape of the Milky Way's Dark Matter halo

Jesus Prada,[1*] Jaime E. Forero-Romero,[1] Volker Springel[2]
[1] Departamento de Fśica, Universidad de los Andes, Cra. 1 No. 18A-10, Edificio Ip, Bogot; Colombia.
[2] Heidelberg Institute for Theoretical Studies, Schloss-Wolfsbrunnenweg 35, D-69118 Heidelberg Germany.

Accepted XXX. Received YYY; in original form ZZZ

ABSTRACT
We measure the shape of the dark matter halos of Milky Way type galaxies.

Key words: keyword1 – keyword2 – keyword3

1 INTRODUCTION

A robust prediction of the Cold Dark Matter (CDM) paradigm is that DM halos are ellipsoidal and can be characterized by the principal axes $a > b > c$. This ellipsoidal shape is mostly due to the anisotropical and clumpy accretion of matter influenced by environmental structures. Numerical studies how that the shape has a strong mass dependence (Allgood et al. 2006), halos are also rounder at the outerskirts than at the inner part. Shape also evolves with cosmic time, halos get rounder as they evolve.

There is however a high degree of uncertainty on what is the degree of uncertainty on the degree of ellipticity of the Milky Way DM halo. This problem has been addressed both by observations and simulations. The difficulty in making an observational measurement lies in the indirect nature of the effect; i.e. the ellipticity can only be constrained by its effects on quantities such as stellar radial velocities. In simulations the uncertainty on predicting the MW DM ellipticity is driven by the different physical effects that should be modeled and its different possible numerical implementations.

Observationally some studies prefer oblate (i.e. a=b>c) configurations at small distances around ≤ 20 kpc (see Law & Majewski 2010; Bovy et al. 2016; Loebman et al. 2012; Olling & Merrifield 2000; Banerjee & Jog 2011) and more triaxial and prolate configurations on the outter distances ≥ 20 kpc (see Vera-Ciro & Helmi 2013; Law et al. 2009; Deg & Widrow 2013; Banerjee & Jog 2011). However, some studies are inclined towards prolate configurations even at the inner parts of the halo (see Bowden et al. 2016), and although it previously seemed that a triaxial DM halo on the outerskirts would be necessary to fully explain the characterization of the Sagittarius stream (Law et al. 2009), recent studies questioned this claim by reporting inconsistencies with narrow stellar streams Pearson et al. (2015) or finding that the relaxation of other constraints may make this claim unnecessary Ibata et al. (2013).

In simulations there is strong evidence claiming that the presence of baryons produces axisymmetrical halos. For instance, some studies have shown that the DM halo shape must be axisymmetrical to ensure the stability of a hydrodynamical disk embeded in a static DM halo. Other have studied this rounding effect by simulating the disk as rigid potential inside an N-body triaxial DM halo Debattista et al. (2008); Debattista et al. (2013); Kazantzidis et al. (2010) finding that the halo responds to the disk by becoming less triaxial.

The caveat of the studies mentioned above is that they do not follow baryons in the whole cosmological context. Other studies overcome this limitation by using resimulations (Abadi et al. 2010; Bryan et al. 2013) finding that the feeback related to star formation in the disk drives the strenght of the round effect. Recently Chua et al. (2018a) made a study in a cosmological simulation to compare the effect of including baryons. They do find, on average, rounder halo shapes once hydrodynamic effects are included, but it is uncertain the strenght of this statistical effect on galaxies similar to the MW.

All these difficulties (enough numerical resolution, explicit cosmological context, appropriate feedback physics to produce realistic MW disks) have limited the studies that want to study the rounding effect of baryons in MW-like galaxies. In this work we overcome all these limitations by analyzing the results of state-of-the-art hydrodynamical simulations of isolated halos that resemble the Milky Way. We also perform a convergence study with simulation performed at different resolution levels and explicitly compare the role of DM only vs. DM+hydro on the MW DM halo shape.

2 NUMERICAL SIMULATIONS

In this work we use the results of the state-of-the art Auriga simulations (Grand et al. 2017). The objects in those simulations were selected from a set of 30 isolated halos in the Evolution and Assembly of GaLaxies and their Environments (EAGLE) project (Schaye et al. 2015). These halos were ran-

* E-mail: jd.prada1760@uniandes.edu.co

Reference	q_ρ	s_ρ	q_ϕ	s_ϕ	R	θ	comment
Olling & Merrifield (2000)	**1.00**	**0.80**			$\simeq$ 8kpc	0°	Method: Stellar dynamics and HI density.
Law et al. (2009)			**0.83**	**0.67**	$\lesssim$ 60kpc	90°	Mid-axis orientation. Method: Sagittarius stream
Law & Majewski (2010)			**0.99**	**0.72**	[20kpc,60kpc]	90°	Mid-axis orientation, Method: Sagittarius stream
Loebman et al. (2012)	**1.00**	**0.47**			$\sim$ 20kpc	0°	Method: SDSS statistics
Deg & Widrow (2013)	0.72	0.28	0.82	0.40	[20kpc,60kpc]	90°	Mid-axis orientation. Method: Sagittarius stream
Vera-Ciro & Helmi (2013)			**1.00**	**0.90**	$\lesssim$ 10kpc	0°	Method: Sagittarius stream & LMC
			0.90	**0.80**	$\gtrsim$ 10kpc	90°	Mid-axis orientation on the outside.
Bovy et al. (2016)	**0.95**	**0.95**			$\lesssim$ 20kpc	90°	Method: Stellar streams
Bowden et al. (2016)			$[\mathbf{0.5, 0.66}]$	$[\mathbf{0.5, 0.66}]$	[5kpc,10kpc]	90°	Weak constraint on prolate halo. Method: SDSS stars dynamics.
Banerjee & Jog (2011)	**1**	**1**			9kpc	0°	Method: HI gas.
	0.5	**0.5**			24kpc	0°	Monotonical change between radial regimes.
Johnston et al. (2005)	**1**	$[\mathbf{0.83 - 0.92}]$			$\lesssim$ 60kpc	0°	Method: Sagittarius stream

Table 1. (TODO: compute analogues in isopotential or isodensity according to Binney and Tremaine)

Reference	q_ρ	s_ρ	q_ϕ	s_ϕ	R	comment
Chua et al. (2018b)	$\mathbf{0.88 \pm 0.10}$	$\mathbf{0.70 \pm 0.11}$			$0.15R_{200}$	Illustris
Bryan et al. (2013)	$[\mathbf{0.84, 0.86}]$	$[\mathbf{0.66, 0.70}]$			R_{200}	For different cosmologies and feedback recipies. Calculated from a fit at $M_\odot = 10^12$
Abadi et al. (2010)			**0.98**	**0.85**	-	Almost independent of radius. No feedback: boundary case

Table 2. (TODO: compute analogues in isopotential or isodensity according to Binney and Tremaine)

domly selected from a sample of the most isolated quartile of halos whose virial mass M_{200} varied between $10^{12}M_\odot$ and $2\times10^{12}M_\odot$. These halos were re-simulated with higher resolution an varying physical realism using the AREPO code (Springel 2010).

All 30 halos were simulated within resolution defined for Aquarius simulations corresponding to $\sim 3\times10^6$ high resolution DM particles of $\sim 2.5\times10^5 M_\odot$. This resolution is labeled as Level 4, the main details for each halo are consigned in Table **??**. From these 30 halos, 6 of them where re-simulated at higher resolution (labeled as Level 3) taking into account a spatial factor of 2 in each dimension. Details of Level 3 halos are in Table **??**. Furthermore, for each halo in each level of resolution there are two versions of the simulation: DM-only and DM plus baryons with magneto-hydrodynamical (MHD) physics.

3 DETERMINING THE HALO SHAPE

There are two main ways to estimate the DM halo shape at a fixed radius: by computing isopotential or isodensity surfaces. Observational inference models estimate the shape from the isopotential contours, while simulations work with the isodensity contours which can be directly calculated from particle positions. However, the density contours are not smooth and are very sensitive to the presence of small satelites. For this reason we choose to measure the shape by taking volume-enclosed particles, rather than shell-enclosed.

We follow the shape measurement method presented by Allgood et al. (2006) that uses the reduced inertia tensor,

$$I_{ij} = \sum_k \frac{x_k^{(i)} x_k^{(j)}}{d_k^2}, \tag{1}$$

with the positions components weighted by the k-th particle distance $d_k^2 = x_k^2 + y_k^2 + z_k^2$, the particle positions are measured from the minimum of the gravitational potential in each halo. The diagonalization of this tensor yields the principal axes of the structure as well as the eigenquantities which are proportional to the squared principal axes $a > b > c$.

We start the calculations taking into account particles within a sphere of radius R and then recharacterize the triaxial parameters by taking into account particles within an ellipsoid of semi-axes $r, r/q, r/s$ and weighted distance $d^2 = x^2 + (y/q)^2 + (z/s)^2$, where $q = b/a$ and $s = c/a$ are the previously calculated axial ratios. We repeat this process until the average deviation of semi-axes is less than 10^{-6}. This is the same method used to estimate the halo shape in the DM-only Aquarius simulations (Vera-Ciro et al. 2011).

We restrict the sampling of the ellipsoidal parameters to radii between $1/16R_{vir}$ and $2R_{vir}$, where R_{vir} is taken as the radius enclosing a sphere with 500 times the average dark matter density of the Universe. All our results use of this reference radius unless strictly stated otherwise. We peform the shape measurements both as a function of radius and redshift for all halos in the sample.

4 RESULTS

4.1 Radial trends

In DM-only simulations halos are monotonically rounder with increasing radius, this confirms results already reported in the literature (Vera-Ciro et al. 2011). Figure 1 illustrates this effect. There we show the DM density of a DM-only halo at redshift zero. The halo is aligned with the minor axis. The ellipsoid shows the outermost boundary of the estimated shape ellipsoid. Formally, this effect is reflected in the axial ratios $b/a, c/a$, which tend to unity on the outerskirts of the halo. As a representative sample of this relations, we show on figure **??** the evolution, for a specific halo, of the axial ratios $b/a, c/a$ and the triaxiality parameter $T = \frac{a^2-b^2}{a^2-c^2}$ in a wide range of radii.

REFERENCES

Abadi M. G., Navarro J. F., Fardal M., Babul A., Steinmetz M., 2010, MNRAS, 407, 435

Allgood B., Flores R. A., Primack J. R., Kravtsov A. V., Wechsler R. H., Faltenbacher A., Bullock J. S., 2006, MNRAS, 367, 1781

Banerjee A., Jog C. J., 2011, ApJ, 732, L8

Bovy J., Bahmanyar A., Fritz T. K., Kallivayalil N., 2016, ApJ, 833, 31

Bowden A., Evans N. W., Williams A. A., 2016, MNRAS, 460, 329

Bryan S. E., Kay S. T., Duffy A. R., Schaye J., Dalla Vecchia C., Booth C. M., 2013, MNRAS, 429, 3316

Chua K. E., Pillepich A., Vogelsberger M., Hernquist L., 2018a, preprint, (arXiv:1809.07255)

Chua K. E., Pillepich A., Vogelsberger M., Hernquist L., 2018b, preprint, (arXiv:1809.07255)

Debattista V. P., Moore B., Quinn T., Kazantzidis S., Maas R., Mayer L., Read J., Stadel J., 2008, The Astrophysical Journal, 681, 1076

Debattista V. P., Roškar R., Valluri M., Quinn T., Moore B., Wadsley J., 2013, MNRAS, 434, 2971

Deg N., Widrow L., 2013, MNRAS, 428, 912

Grand R. J. J., et al., 2017, Monthly Notices of the Royal Astronomical Society, 467, 179

Ibata R., Lewis G. F., Martin N. F., Bellazzini M., Correnti M., 2013, ApJ, 765, L15

Johnston K. V., Law D. R., Majewski S. R., 2005, ApJ, 619, 800

Kazantzidis S., Abadi M. G., Navarro J. F., 2010, ApJ, 720, L62

Law D. R., Majewski S. R., 2010, The Astrophysics Journal, 714, 229

Law D. R., Majewski S. R., Johnston K. V., 2009, The Astrophysical Journal Letters, 703, L67

Loebman S. R., Ivezić Ž., Quinn T. R., Governato F., Brooks A. M., Christensen C. R., Jurić M., 2012, ApJ, 758, L23

Olling R. P., Merrifield M. R., 2000, MNRAS, 311, 361

Pearson S., Küpper A. H. W., Johnston K. V., Price-Whelan A. M., 2015, ApJ, 799, 28

Schaye J., et al., 2015, Monthly Notices of the Royal Astronomical Society, 446, 521

Springel V., 2010, Monthly Notices of the Royal Astronomical Society, 401, 791

Vera-Ciro C., Helmi A., 2013, ApJ, 773, L4

Vera-Ciro C. A., Sales L. V., Helmi A., Frenk C. S., Navarro J. F., Springel V., Vogelsberger M., White S. D. M., 2011, MNRAS, 416, 1377

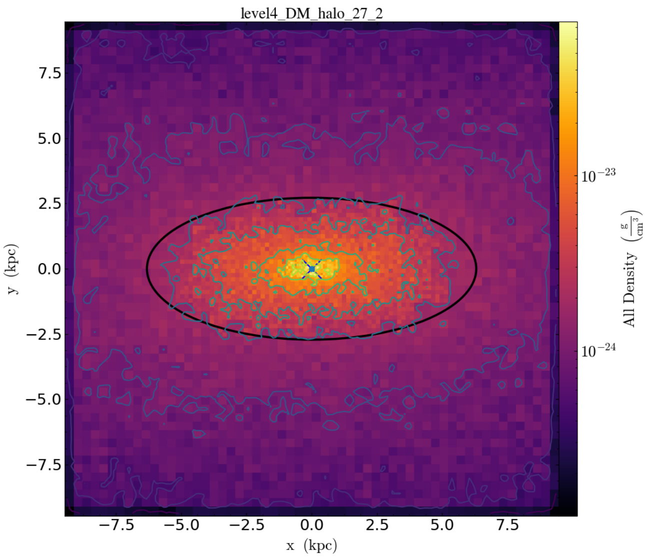

(a) halo 27 DM shape at small radius

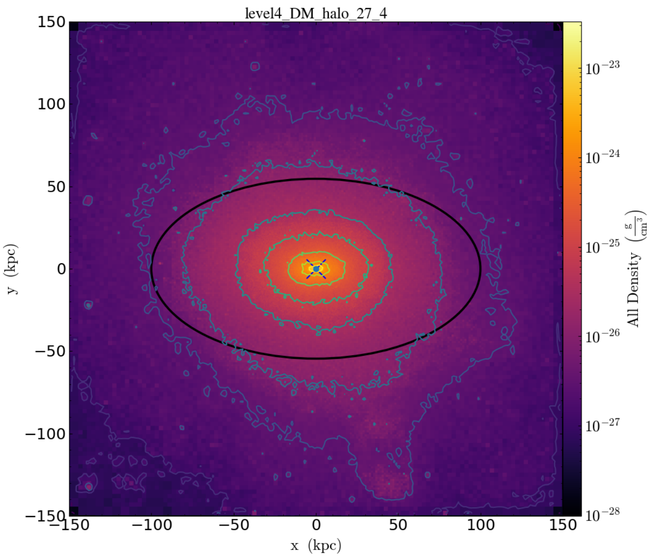

(b) halo 27 DM shape at big radius

Figure 1. DM density for inner/outer (left/right panel) DM halo regions.